Article

Synthesis of Thermoplastic Starch-Bacterial Cellulose Nanocomposites via *in situ* Fermentation

Marlon A. Osorio,[a] David Restrepo,[a] Jorge A. Velásquez-Cock,[a] Robin O. Zuluaga,*,[b] Ursula Montoya,[b] Orlando Rojas,[c] Piedad F. Gañán,[a] Diana Marin[d] and Cristina I. Castro[e]

[a]Facultad de Ingeniería Química and [b]Facultad de Ingeniería Agroindustrial, Universidad Pontificia Bolivariana, Circular 1°, No. 70-01, Medellín, Colombia

[c]Department of Forest Biomaterials, North Carolina State University, Campus Box 8005, Raleigh, North Carolina 27695-8005, USA and Faculty of Chemistry and Materials Sciences, Department of Forest Products Technology, Aalto University, P.O. Box 16300, FI-00076 Aalto, Finland

[d]Ecomaterials Group, National Research Institute of Materials Science and Technology (INTEMA), National Research Council (CONICET), National University of Mar del Plata (UNMdP), Av. Juan B. Justo 4302, B7608FDQ Mar del Plata, Argentina

[e]Facultad de Ingeniería Textil, Universidad Pontificia Bolivariana, Circular 1°, No. 70-01, Medellín, Colombia

Neste trabalho são apresentados os resultados da síntese de nanocompósitos baseados em amido termoplástico (TPS) reforçado com nanofitas de celulose bacteriana (BC). A síntese foi feita por fermentação *in situ* e formação de ligações cruzadas. A fermentação para a obtenção das nanofitas foi conduzida por sete dias empregando a bactéria colombiana nativa *Gluconacetobacter medellinenses*; os nanocompósitos foram plasticizados com glicerol e as ligações cruzadas foram formadas com ácido cítrico. Os nanocompósitos obtidos depois destes sete dias de fermentação foram caracterizados por análise termogravimétrica (TGA), espectroscopia na região do infravermelho com transformada de Fourier com refletância total atenuada (FTIR-ATR) e microscopia electrônica de varredura (SEM). Observou-se que, ao longo da fermentação, a porcentagem de reforço nos nanocompósitos permaneceu constante. Os novos nanocompósitos TPS/BC apresentaram uma forte adesão interfacial e uma maior estabilidade térmica e aquosa, assim como propriedades mecânicas melhoradas. Os resultados obtidos aumentam consideravelmente as possibilidades de aplicação do amido na indústria de embalagens.

In this paper, a nanocomposite based on thermoplastic starch (TPS) reinforced with bacterial cellulose (BC) nanoribbons was synthesized by *in situ* fermentation and chemical crosslinking. BC nanoribbons were produced by a Colombian native strain of *Gluconacetobacter medellinensis*; the nanocomposite was plasticized with glycerol and crosslinked with citric acid. The reinforcement percentage in the nanocomposites remained constant throughout the fermentation time because of the TPS absorption capability of the BC network. Nanocomposites produced after fermentation for seven days were characterized using thermogravimetric analysis (TGA); Fourier transformed infrared spectroscopy with attenuated total reflectance (FTIR-ATR), mechanical testing and scanning electron microscopy (SEM). The new TPS/BC nanocomposites exhibit strong interfacial adhesion, improved thermal behavior, water stability and enhanced mechanical properties. These findings support the applications of starch in the packaging industry.

Keywords: nanocomposite, thermoplastic starch, bacterial cellulose, *in situ* fermentation, chemical crosslinking

*e-mail: robin.zuluaga@upb.edu.co

Introduction

Currently, the use of renewable resources is becoming more prominent because of the inherent beneficial impacts in the agricultural, economic and environmental fronts.[1] In the packaging industry, biopolymers, such as polylactic acid, starch and cellulose, are replacing traditional synthetic polymers at increased levels, for example, in diverse products that include optically transparent cellulose nanocomposites[2] and antimicrobial starch films.[3] In fact, starch and cellulose are widely available polymers that can be obtained at low cost and are biodegradable;[4,5] they consist of glucose units linked by β-1,4- and α-1,4-glycosidic bonds, respectively.[6]

Thermoplastic starch (TPS) is one of the most useful and promising materials in packaging.[7] In TPS plasticizers, such as water or glycerol, are introduced to facilitate the disruption of intermolecular chain interactions[7] that otherwise impart native starch with a melting point temperature that is substantially higher than its decomposition temperature. Ethylene glycol and urea,[8] as well as certain sugars, such as sorbitol,[9] fructose, glucose, mannose, and galactose,[10] have also been successfully used as the plasticizer agent.

Efforts in TPS synthesis are mainly directed to increasing its mechanical properties, reducing the viscosity and enhancing the casting performance for easier TPS processing. These efforts are required because TPS derivatives are frequently brittle and water-sensitive,[11] which are features related to the random growth of amylose crystals.[12] Recently, nanocomposites reinforced with cellulose nanofibers were developed to address a number of the issues indicated above.[4,6,11]

A good interphase is expected between cellulose and starch, given their similar structures.[6] However to achieve high nanocomposite strength, good dispersion between the constituent elements is important. This condition also limits the water uptake capacity of starch and its macromolecular reorganization.[1] For these reasons, *in situ* self-assembly techniques[13] are the most appropriate processes to obtain thermoplastic starch nanocomposites, especially because the web-like network of BC is maintained using such tecniques.[14]

Gluconacetobacter sp genus bacteria can produce self-assembled nanocomposites of bacterial cellulose (BC) by *in situ* fermentation.[15,16] This process enables the formation of BC nanocomposites with bioactive agents and synthetic monomers, as well as polymers, metals and metal oxides.[17] The primary subject the present investigation is the use of TPS as the polymer matrix in the *Gluconacetobacter* culture media to produce nanocomposites.

Crosslinking is used to enhance the mechanical properties and water stability of starch by covalent bond formation during the process.[18] Scheme 1 shows the crosslinking reaction with carboxylic acid; the first step is the molecular dehydration of the acid followed by the reaction of esterification. This mechanism was proposed for cellulose, but the research results of Reddy and Yang[18] suggest that it also applies to starch.

The primary scientific contribution of this paper is the use of a Colombian native bacterium (*Gluconacetobacter medellinensis*)[19] in the development of *in situ* TPS/BC nanocomposites using the bioengineering capability of the microorganism followed by chemical crosslinking.

Experimental

Materials

Potato starch, composed of amylose (32.8%) and amylopectin (67.1%), was provided by Almicor Industries
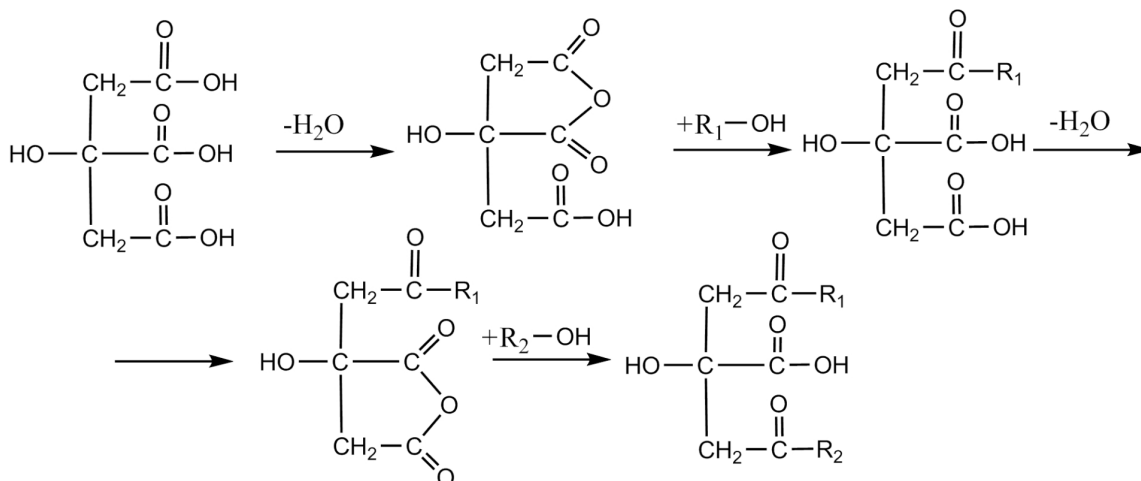
Scheme 1. Chemical crosslinking using carboxylic acids, where R_1 and R_2 can be either cellulose or starch.

Ltd. (Bogota, Colombia). USP grade glycerol was provided by Protokimica (Medellin, Colombia). Analytical grade citric acid, Na_2HPO_4, NaH_2PO_4, peptone, yeast extract and glacial acetic acid were supplied by Laboratorios Ltda. (Medellin, Colombia); all the reagents used are not toxic to the bacteria.

In situ nanocomposite synthesis

To synthesize the nanocomposites *in situ*, 500 g of Hestrin and Schramm culture medium (HS)[20] was used, and the following components were added: starch (4%) as the matrix of the nanocomposite, glycerol (2%) as the plasticizer, citric acid (0.24%) as the crosslinking agent and NaH_2PO_4 (0.12%) as the catalyst of the chemical crosslinking.[18] The pH was adjusted to 3.6 with glacial acetic acid. Next, the culture medium was placed on a heating plate at 90 °C (20 minutes, 1500 rpm) to achieve the first starch gelatinization. Finally, the broth was inoculated with a recently isolated strain of *Glucanacetobacter medellinensis* (15%).[19] Fermentation was performed at room temperature throughout 7, 10 and 13 days for different samples in static flasks of 80 g each.

A neat matrix was also prepared as a control. In this case, the culture medium was prepared as indicated above for the nanocomposite, and 25 g of the inoculated broth was subsequently placed on Petri dishes (10 cm diameter); finally, the crosslinking of the nanocomposite and the neat TPS matrix was performed, as mentioned in the next section.

Nanocomposite and neat matrix chemical crosslinking

At the end of the fermentation, the respective system was removed from the culture medium and then was crosslinked with citric acid and NaH_2PO_4 as catalyst. The procedure was performed as follows: the films were transferred to an oven at 50 °C for 48 h, and then they were hot pressed (2000 psi) at 165 °C for 5 minutes.[18]

Dry weight of the nanocomposites

The production of cellulose by the bacteria and the amount of reinforcement in the nanocomposites were determined at the end of the fermentation. Six fermentations were performed: three were used to determine the weight of the final nanocomposite, and the other three were used to determine the amount of cellulose in the nanocomposites after fermentation. Non-crosslinked nanocomposite samples (NCS) were immersed in 5% KOH solution for 14 h and rinsed to neutral pH with distilled water to

solubilize the starch, peptone and other compounds of the culture medium, leaving the nanocellulose film from which the cellulose amount was determined gravimetrically. This weight was taken as the amount of reinforcement. The same procedure was performed to evaluate the effect of the presence of the different additives in BC production at 7, 10 and 13 days.

Qualitative solubility test

NCS and crosslinked samples (CS) were placed in containers with 500 mL of distilled water under static conditions for 48 h. To evaluate the crosslinking grade, water was frequently changed, and images of the systems were collected to monitor the progress of solubilization.

Thermal properties

Thermogravimetric analyses were performed by using a Mettler Toledo TGA/SDTA 851e instrument in a nitrogen atmosphere at 40 mL min^{-1} and a heating rate of 10 °C min^{-1}. The samples were heated from 30 to 800 °C.

Infrared spectroscopy

Infrared spectroscopy experiments were performed using a Fourier transform infrared (FTIR) Nicolet 6700 series spectrometer equipped with a single-reflection attenuated total reflectance (ATR) and a type IIA diamond mounted tungsten carbide. The diamond ATR had an approximate sampling area of 0.5 mm^2 and applied a consistent, reproducible pressure to every sample. The infrared spectra were collected with a 4 cm^{-1} resolution, and 64 scans were performed.

Mechanical properties of the nanocomposites

Young's modulus and tensile strength were determined for nanocomposite samples produced after seven fermentations days (NCS and CS), as well for the neat matrix and the reinforcement (TPS and BC). The mechanical properties were evaluated with tensile tests performed in an Instron 5582 Universal Testing Instrument, equipped with a 50 N load cell, with a crosshead speed of 25 mm min^{-1}. Six repetitions were performed per sample using rectangular strips (5 mm × 19 mm).

Scanning electron microscopy (SEM) of nanocomposites

SEM was used to study the morphology of samples after cryo-fracture. The samples were coated with gold/

palladium using an ion-coater and imaged with a Jeol JSM 5910 LV microscope operated at 10 kV.

Results and Discussion

BC production in a TPS-modified culture media

The weights of cellulose (dry basis) produced at 13 fermentation days in an HS medium (0.32 ± 0.01 g) and in an HS medium modified with TPS (0.21 ± 0.06 g) were compared. A total weight reduction of 33% was noted when the culture media was modified with TPS; this effect is explained by the fact that TPS increases the viscosity and limits the molecular diffusivity of oxygen in the aqueous phase.[21]

The BC production increases with time in an HS medium modified with TPS. The highest cellulose production was obtained at 13 days of fermentation; however, the amount of cellulose with respect to the TPS in the final materials was maintained, regardless of the fermentation time. Consequently, the weight percentage of reinforcement remains fairly constant throughout the fermentation (Table 1).

Table 1. Nanocomposite reinforcement

Fermentation time / day	W_{CS} / g, dry basis	W_{BC} / g, dry basis	BC / %
7	0.97 ± 0.13	0.16 ± 0.01	16.60 ± 1.53
10	1.01 ± 0.10	0.17 ± 0.01	17.02 ± 0.62
13	1.16 ± 0.18	0.22 ± 0.01	18.76 ± 2.21

This effect is explained by the tendency of BC to absorb the matrix in the growing network.[22] For subsequent analysis, the nanocomposites obtained after seven fermentation days were used, which incorporated 16.6 ± 1.5% of BC. Prior to seven days of fermentation, no significant BC growth was noticeable.

Qualitative solubility test

Photographic images were used to verify the chemical crosslinking of TPS after immersion in distilled water.

Figures 1a and 1b show the NCS and CS, respectively, after 5 h water rinsing, and Figures 1c and 1d show the NCS and CS, respectively, after 48 h rinsing.
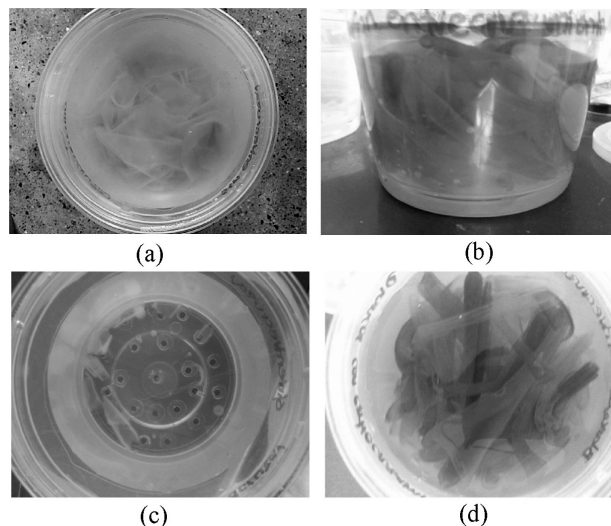

Figure 1. Photographs for qualitative analysis of the NCS and the CS: (a) NCS after 5 h rinsing; (b) CS after 5 h rinsing; (c) NCS after 48 h rinsing; and (d) CS after 48 h rinsing.

A considerable amount of the NCS was solubilized after 5 h. After 48 h, only a small residual solid amount was observed. The CS remains unchanged during the test, even after 48 h rinsing with distilled water. These results confirm the need for crosslinking to create covalent bonds in the matrix and reduce the water sensitivity, thereby increasing the mechanical strength of the nanocomposites,[18] as will be discussed later.

Thermal properties of the nanocomposites

The thermal properties of the nanocomposites are summarized in the Table 2 for all the samples according to three main degradation events.

The first thermal event corresponds to water evaporation/dehydration, which begins immediately after the temperature is increased and finishes at approximately 100 °C. The weight loss percentage in this event is dependent on the moisture

Table 2. Thermal behavior of nanocomposites and their components

Thermal event	Variable	Sample			
		TPS	BC	CS	NCS
1st	Maximal decomposition temperature / °C	80.5	81.5	81.4	80
	Weight loss / %	3.2	3.9	3.2	3.9
2nd	Maximal decomposition temperature / °C	146	–	128.3	157.8
	Weight loss / %	10.7	–	6.7	16.9
3rd	Maximal decomposition temperature / °C	282	298.4	301.4	293.7
	Weight loss / %	44.5	32.1	39.1	45.9

content of each sample.[6,7,13] The second event corresponds to glycerol decomposition,[23,24] which is common for all the samples, excluding the BC ones.

The third thermal event is due to the starch/cellulose decomposition, including depolymerization phenomena and the degradation of the glucopyranose units and their subsequent oxidation.[4] This decomposition occurs at 280 °C for TPS, 290 °C for NCS and 300 °C for the BC and CS nanocomposites. A thermal decomposition of TPS (from potato starch) was reported to occur at approximately 291 °C.[9] Martins *et al.* reported a thermal decomposition for TPS at 327 °C; these authors also described an enhancement of the thermal stability of TPS, by 10 °C, if reinforced *ex situ* with BC.[11] In the present study, the increase of the temperature is approximately 20 °C, due to an enhanced reinforcement capability resulting from the *in situ* method of fabrication, thereby offering an advantage as far as the improved thermal stability.[25] For TPS, the thermal degradation temperature is shifted to higher temperatures upon incorporation of BC. Recently, Montoya *et al.* and Soykeabkaew *et al.* reported this behavior when TPS was reinforced with BC.[6,23]

Infrared spectroscopy

No distinctive differences were observed for the spectra of the nanocomposites (CS and NCS) and the TPS because they are comprised over of 83% of starch (see Figure 2).
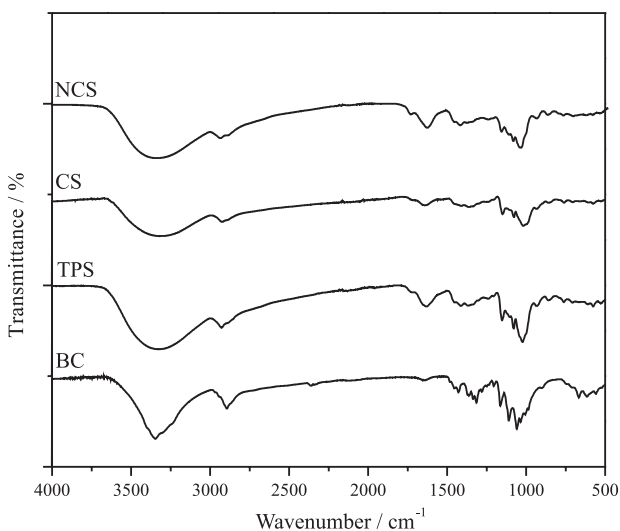

Figure 2. FTIR-ATR spectra of nanocomposites and their components.

In comparison with BC, the nanocomposites exhibit two differentiated zones: one from 3750 to 2750 cm^{-1} and another one from 2000 to 500 cm^{-1}. In the first zone, a wide band centered between 3500 and 3250 cm^{-1} is observed, whereas the BC exhibits a narrow band at 3340 cm^{-1}.

These peaks represent stretching of the hydroxyl groups, which contribute to the vibratory complex associated to the inter- and intra-molecular bonds of the hydroxyl groups and are the basic structures for starch and for cellulose.[26] In the nanocomposites, these bands are superimposed, and the wide band of starch masks the narrow band of cellulose.

In the second zone, between the bands of 1500 and 1330 cm^{-1}, the nanocomposites exhibit well-defined peaks due to the stretching of the CH, CH$_2$ and –OH groups.[13]

For CS, the crosslinking process is shown in the peaks centered at 1724 cm^{-1} due to the carboxyl and ester carbonyl bands;[18] however, because all samples contain citric acid, which vibrate at the same band, the crosslinking process is hidden by its vibration. To confirm the chemical crosslinking, both qualitative solubility and mechanical tests were performed. The band at 1046 cm^{-1} is common for all the samples, corresponding to the C–O stretching of the C–OH in carbohydrates.[26,27]

Mechanical properties of the nanocomposites

Figure 3 shows the results for the tensile strength (Figure 3a), Young's modulus (Figure 3b) and the strain at break (Figure 3b) of the nanocomposites.

The crosslinked nanocomposite (CS) exhibits a tensile strength four times higher (5.65 ± 1.36 MPa) than for TPS (1.26 ± 0.05 MPa), whereas for the non-crosslinked nanocomposites (NCS) it is only three times higher (3.54 ± 0.39 MPa) than for TPS. Young's modulus is also enhanced: 715.82 ± 56.84 MPa for CS compared to 1.85 ± 0.15 MPa for TPS, i.e., ca. 400 times higher. Montoya *et al.* recently reported a tensile strength of 7.8 ± 0.7 MPa and a Young's modulus of 247 ± 29.4 MPa using *ex situ* BC reinforcement.[6] Moreover, Kaushik *et al.* reported a tensile strength of 6.75 MPa and a Young's modulus of 230 MPa; in this case, they processed *ex situ* cellulose nanofibers from wheat straw.[28] The *in situ* processing has the advantage of enhancing the Young's modulus compared with the *ex situ* process.[25] Nakagaito *et al.*[29] confronted Young's modulus of phenol-formaldehyde/BC (*in situ*) nanocomposites against phenol-formaldehyde/microfibrillated BC ones (*ex situ*), and found that the Young's modulus was significantly higher, with a value of 28 GPa compared to 19 GPa for fibrillated pulp nanocomposites. The superior modulus value was attributed to the uniform, continuous, and straight nanoscale network-like cellulosic elements oriented in plane via the compression of BC pellicles.[29]

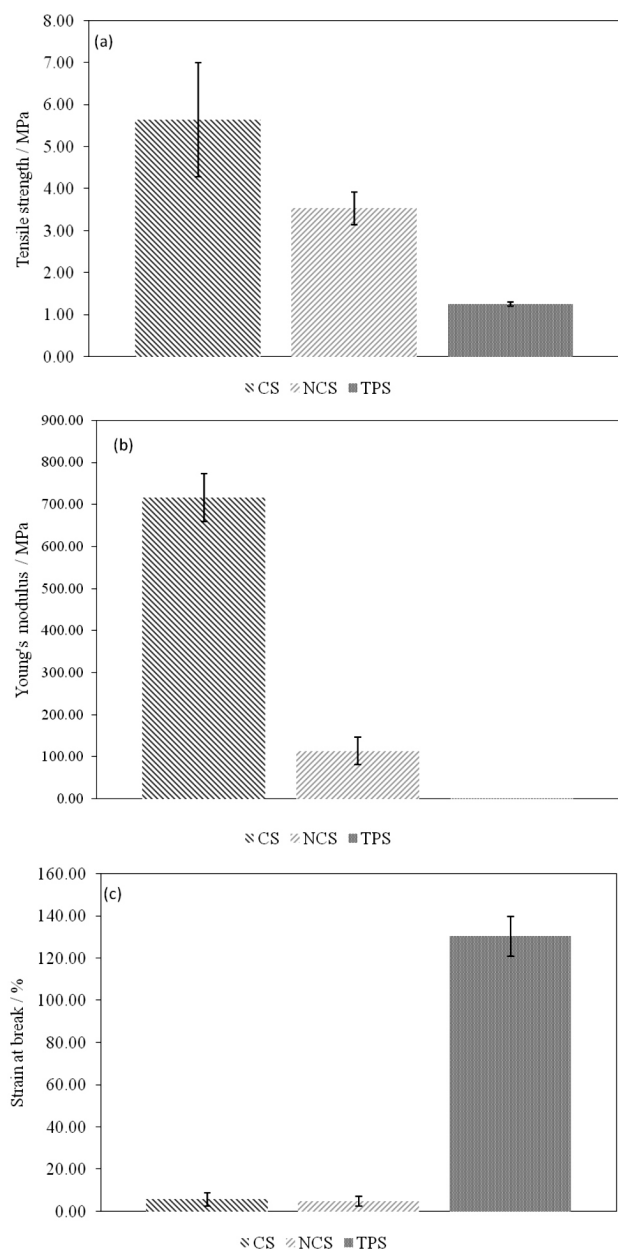Chemical crosslinking also increases the mechanical behavior of the nanocomposites; CS exhibits a tensile

Woehl *et al.* found similar results when BC cellulose was incorporated to a TPS matrix.[11,30]

Scanning electron microscopy (SEM) of the nanocomposites

Figure 4 shows the morphologies of the cryo-fracture surface of the nanocomposites and their components.
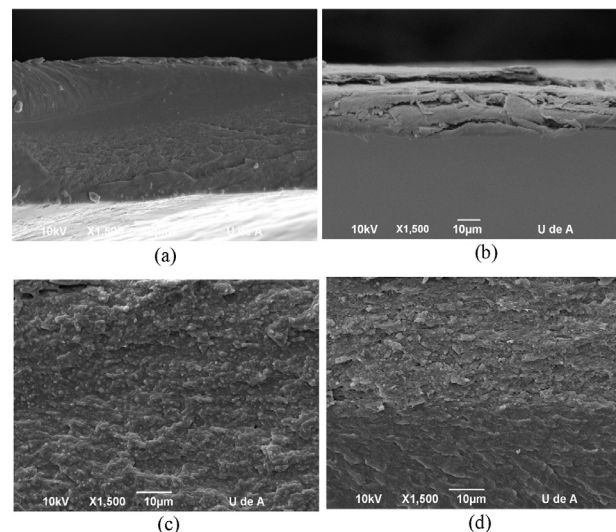

Figure 4. Scanning electron microscopy images of: (a) TPS; (b) BC; (c) NCS; and (d) CS.

The fractured TPS surface (Figure 4a) was smooth without pores or cracks.[31] For the BC (Figure 4b), a typical delamination is observed.[32] For the nanocomposites of NCS and CS (Figures 4c and 4d, respectively), this observation is absent, indicating that the BC ribbons were homogeneously distributed through the matrix, acting as glue between BC layers in the nanocomposites. Likewise, the absence of pull-out BC ribbons demonstrates the strong interfacial adhesion between BC and the TPS matrix, and the lack of agglomerates demonstrates a good dispersion of the filler in the matrix. All of the above data provides a good indication of the structural integrity of the nanocomposite, in agreement with the increase in the mechanical properties of the matrix due to the presence of BC network as well as the *in situ* nanocomposite processing and chemical crosslinking, as discussed previously.[31-33]

Conclusions

A new nanocomposite was developed with a TPS matrix and bacterial cellulose as reinforcement using *in situ* processing and the bioengineering capability of a native strain of *Glucanacetobacter medellinensis*. The nanocomposite was plasticized with glycerol and crosslinked with citric acid; the improvement of the water

Figure 3. Mechanical properties of the nanocomposites: (a) tensile strength; (b) Young's modulus; and (c) strain at break.

strength and Young's modulus 1.6 and 6.3 times higher than those for NCS, respectively (see Figures 3a and 3b). These values can be attributed to the effective stress transfer through the specimen because of the network formation after crosslinking.[1,18]

Chemical crosslinking does not affect significantly the strain at break, Reddy and Yang and Jiugao *et al.* observed that this process enhances the strain at break of TPS,[18,24] but according to Figure 3c, this effect was not clearly observed; however, the BC incorporation caused a considerable decrease in the elongation at break, up to ca. 125% for the NCS and CS. Researchers such as Martins *et al.* and

stability and the enhancement of the mechanical properties of the CS confirm that the chemical crosslinking reaction (see Scheme 1) occurred.

The nanocomposites exhibited a strong interfacial adhesion. The *in situ* BC reinforcement and chemical crosslinking allowed a higher thermal stability and improved the mechanical behavior of the nanocomposites compared to TPS (tensile strength of 5.7 ± 1.4 MPa and Young's modulus of 715.8 ± 56.8 MPa) because of the addition of *in situ* network-like nanoribbons and the formation of covalent bonds. According to these findings, it is concluded that the observed properties enable further applications of starch, such as packaging.

Supplementary Information

Supplementary data are available free of charge at http://jbcs.sbq.org.br as PDF file.

Acknowledgments

References

1. Kumar, A. P.; Singh, R. P.; *Bioresour. Technol.* **2008**, *99*, 8803.

2. Abdul Khalil, H. P. S.; Bhat, A. H.; Ireana Yusra, A. F.; *Carbohydr. Polym.* **2012**, *87*, 963.

3. Joerger, B. R. D.; *Packag. Technol. Sci.* **2007**, *20*, 231.

4. Teixeira, E. D. M.; Pasquini, D.; Curvelo, A.; Corradini, E.; Belgacem, M. N.; Dufresne, A.; *Carbohydr. Polym.* **2009**, *78*, 422.

5. Abe, K.; Yano, H.; *Cellulose* **2009**, *16*, 1017.

6. Montoya, Ú.; Zuluaga, R.; Castro, C.; Goyanes, S.; Gañán, P.; *J. Thermoplast. Compos. Mater.* **2012**, *27*, 413.

7. Mościcki, L.; Mitrus, M.; Wójtowicz, Ag.; Oniszczuk, T.; Rejak, A.; Janssen, L.; *Food Res. Int.* **2012**, *47*, 291.

8. Da Roz, A.; Carvalho, A. J.; Gandini, A.; Curvelo, A. A.; *Carbohydr. Polym.* **2006**, *63*, 417.

9. Cyras, V. P.; Manfredi, L. B.; Ton-That, M.-T.; Vázquez, A; *Carbohydr. Polym.* **2008**, *73*, 55.

10. Zhang, Y.; Han, J. H.; *J. Food Sci.* **2006**, *71*, 253.

11. Martins, M. G.; Magina, S. P.; Oliveira, L.; Freire, C.; Silvestre, A.; Neto, C.; Gandini, A.; *Compos. Sci. Technol.* **2009**, *69*, 2163.

12. Azeredo, H. M. C. D.; *Food Res. Int.* **2009**, *42*, 1240.

13. Brown, E. E.; Laborie, M.-P. G; *Biomacromolecules* **2007**, *8*, 3074.

14. Huang, H.-C.; Chen, L.-C.; Lin, S.-B.; Hsu, C.-P.; Chen, H.-H; *Bioresour. Technol.* **2010**, *101*, 6084.

15. Castro, C.; Zuluaga, R.; Álvarez, C.; Putaux, J.-L.; Caro, G.; Rojas, O.; Mondragon, I.; Gañán, P.; *Carbohydr. Polym.* **2012**, *89*, 1033.

16. Castro, C.; Vesterinen, A.; Zuluaga, R.; Putaux, J.-L.; Caro, G.; Filpponen, I.; Rojas, O.; Kortaberria, G.; Gañán, P.; *Cellulose* **2014**, *21*, 1745.

17. Klemm, D.; Schumann, D.; Kramer, F.; Heßler, N.; Koth, D.; Sultanova, B.; *Macromol. Symp.* **2009**, *280*, 60.

18. Reddy, N.; Yang, Y.; *Food Chem.* **2010**, *118*, 702.

19. Castro, C.; Trcek, J.; Zuluaga, R.; De Vos, P.; Caro, G.; Aguirre, R.; Putaux, J.-L.; Gañán, P.; *Int. J. Syst. Evol. Microbiol.* **2013**, *63*, 1119.

20. Schramm, M.; Hestrin, S.; *J. Gen. Microbiol.* **1954**, *11*, 123.

21. Kilonzo, P. M.; Margaritis, A.; *Biochem. Eng. J.* **2004**, *17*, 27.

22. Laborie, M.-P. In *The Nanoscience and Technology of Renewable Biomaterials*; Lucian, A. L.; Orlando, J. R.; eds.; John Wiley & Sons: Chichester, USA, 2009, ch. 9.

23. Soykeabkaew, N.; Laosat, N.; Ngaokla, A.; Yodsuwan, N.; Tunkasiri, T.; *Compos. Sci. Technol.* **2012**, *72*, 845.

24. Jiugao, Y.; Ning, W.; Xiaofei, M.; *Starch/Staerke* **2005**, *57*, 494.

25. Koczak, M. J.; Premkumar, M. K.; *JOM* **1993**, *45*, 44.

26. Gea, S.; Reynolds, C. T.; Roohpour, N.; Wirjosentono, B.; Soykeabkaew, N.; Bilotti, E.; Peijs, T.; *Bioresour. Technol.* **2011**, *102*, 9105.

27. Vigneshwaran, N.; Ammayappan, L.; Huang, Q.; *Appl. Nanosci.* **2011**, *1*, 137.

28. Kaushik, A.; Singh, M.; Verma, G.; *Carbohydr. Polym.* **2010**, *82*, 337.

29. Nakagaito, A. N.; Iwamoto, S.; Yano, H.; *Appl. Phys. A: Mater. Sci. Process.* **2005**, *80*, 93.

30. Woehl, M. A.; Canestraro, C. D.; Mikowski, A.; Sierakowski, M. R.; Ramos, L. P.; Wypych, F.; *Carbohydr. Polym.* **2010**, *80*, 866.

31. Grossmann, E.; Garcia, M. A.; Martino, M. N.; Victo, M.; Zaritzky, N. E;. *Carbohydr. Polym.* **2002**, *50*, 379.

32. Dammström, S.; Salmén, L.; Gatenholm, P.; *Polymer* **2005**, *46*, 10364.

33. Grande, C. J.; Torres, F. G.; Gomez, C. M.; Troncoso, O. P.; Josep, C.; *Polym. Polym. Compos.* **2008**, *16*, 181.